Miniaturized Microstrip Suppressing Cell with Wide Stopband

M. Hayati [1,2], F. Shama [2], and M. Ekhteraei [3]

[1] Department of Electronics, Kermanshah Branch, Islamic Azad University, Kermanshah, Iran
Mohsen_hayati@yahoo.com

[2] Department of Electronics, Razi University, Tagh-E-Bostan, Kermanshah-67149, Iran
f.shama@aut.ac.ir

[3] Young Researchers and Elite Club, Kermanshah Branch, Islamic Azad University, Kermanshah, Iran
m.ekhteraei.ir@ieee.org

Abstract ─ In this paper, based on simple stepped impedance structures a methodology is followed to design a very compact size lowpass filter (LPF) as a suppressing cell. The proposed suppressing cell consists of stepped impedance ladder-type resonators, which provides a wide stopband by creating the transmission zeros to its frequency response. The proposed suppressing cell has clear advantages like low insertion loss in the passband and suitable roll-off. The designed LPF is fabricated on a microstrip layout and tested. The measured results highlight the efficiency of the filter and have a good agreement with the simulated results. With mentioned expression, the fabricated LPF can be a powerful block as a suppressing cell to implement in the distributed high frequency circuits.

Index Terms ─ Lowpass filter, microstrip, miniaturized, stepped impedance structure, suppressing cell.

I. INTRODUCTION

Design of the high frequency circuits are highly extended and demanded, in the modern technologies. Handset devices and wireless communications depend on the high frequency circuits and the suppression of the spurious signals is an important requirement in this field [1]. The position of the lowpass filters is undeniable in order to block and suppress the unwanted harmonics. From the introducing of microstrip technology until now, many microstrip structures and many methods have been presented to design the high efficient LPFs [1-14]. Planar structures are widely used for their simple fabrication and design in [1-13], which have sharp transition band and wide stopband, but these LPFs suffers from the big size, which makes them inappropriate as the suppressing cells to use in hybrid high frequency circuits, in addition to their almost low attenuation levels in their stopbands.

A miniaturized LPF with very sharp roll-off has been designed to eliminate the unwanted harmonics for a Wilkinson power divider in [14], which has a so narrow stopband bandwidth. In [15], using defected ground structures (DGS), an Elliptic-function LPF has been fabricated with sharp roll-off, this technique design not only is not easy to implement but also has disadvantages such as large circuit size and narrow stopband width. A lowpass filter has been designed in [16] with sharp roll-off as a miniaturized LPF, but it is not so compact and has a very narrow rejection bandwidth. In [17], the fabricated LPF has a compact structure, although the stopband region is not wide enough. A wide stopband LPF has been presented in [18], but this filter suffers from its high insertion loss in the passband and its large circuit size. In [19-24], the low value of maximum variation of the group delay in the passband has been introduced as an effective factor in LPF designs, which it tried to be improved in the proposed work. Also, the simple geometry and topology of the designed filter is a significant specification, which can be effective in fabrication and implementation. Therefore the design of a simple structure and high efficient LPF is the main objective of this paper.

In this paper, using stepped impedance microstrip stubs and ladder-type structures, a miniaturized LPF with good rejection bandwidth is designed. The LPF has - 3 dB cut-off frequency at 4 GHz. The rejection band is achieved from 5 to 23.3 GHz. A simple methodology is used to design this filter that follows in the next session. All the simulations are done using Agilent Advanced Design System (ADS) software, and all of the microstrip layouts are designed and fabricated on RT/Duriod5880 substrate with dielectric constant (ε_r) of 2.22, the thickness of 0.508 mm and the loss tangent of 0.0009.

Submitted On: May 26, 2016
Accepted On: August 9, 2016

II. SUPPRESSING CELL DESIGN

At the first step, Elliptic function resonator layout has been selected and expanded using high and low impedance lines, as shown in Fig. 1. The physical lengths of the low-impedance and high-impedance lines are calculated using below equations [10]:

$$L_i = \frac{g_i Z_0}{2\pi f_c g_0}, \tag{1}$$

$$C_i = \frac{g_i g_0}{2\pi f_c Z_0}, \tag{2}$$

$$d_{L_i} = \frac{\lambda g_{L_i}}{2\pi} sin^{-1}\left(\frac{2\pi f_c L_i}{Z_{0L}}\right), \tag{3}$$

$$d_{c_i} = \frac{\lambda g_{c_i}}{2\pi} sin^{-1}(2\pi f_c C_i Z_{0c}), \tag{4}$$

where, Z_{0Ci} and Z_{0Li} are corresponded to the impedance transmission lines with low and high impedance, respectively. g_i and go are the element values of each part of the prototype layout, λ_{gLi} and λ_{gCi} are the guided wavelengths of high and low impedance lines, respectively. With considering the Fig. 1, the ABCD matrix for the proposed resonator can be written as:

$$\begin{bmatrix} A & B \\ C & D \end{bmatrix} = \begin{bmatrix} 1 & \frac{Z_{oc3}}{2} \\ 0 & 1 \end{bmatrix} \times \begin{bmatrix} 1 & 0 \\ Y_{oc1}+Y_{oc2}+Y_{oL1}+Y_{oL2} & 1 \end{bmatrix} \times \begin{bmatrix} 1 & \frac{Z_{oc3}}{2} \\ 0 & 1 \end{bmatrix}, \tag{5}$$

where, $Y_{oc1}, Y_{oc2}, Y_{oL1}$ and Y_{oL2} are the admittances of the high and low impedance transmission lines, which are indicted in Fig. 1.With calculation, the Equation (5) can be simplified in:

$$\begin{bmatrix} A & B \\ C & D \end{bmatrix} = \begin{bmatrix} 1 & Z_{oc3} \\ 0 & 1 \end{bmatrix} \times \begin{bmatrix} 1 & 0 \\ Y_T & 1 \end{bmatrix} = \begin{bmatrix} 1+Z_{oc3}Y_T & Z_{oc3} \\ Y_T & 1 \end{bmatrix}, \tag{6}$$

where, $Y_T = Y_{oc1} + Y_{oc2} + Y_{oL1} + Y_{oL2}$.

The proposed resonator has a symmetric shape as illustrated in Fig. 1; so clearly, it is expected that the resonator must have a reciprocal response. Therefore, the determinant of the ABCD matrix must be equal to 1. The determinant of the ABCD matrix can be calculated from Equation 6 as:

$$\Delta \begin{bmatrix} A & B \\ C & D \end{bmatrix} = 1 + Z_{oc3}Y_T - Z_{oc3}Y_T = 1. \tag{7}$$

Then, the Equation (7) validates the achieved ABCD matrix of the proposed resonator. The simulated S-parameters of the proposed resonator are shown in Fig. 2. As considered, in the passband the resonator has a transmission pole at 2.87 GHz with attenuation level of -15.6 dB and in the stopband the resonator has a transmission zero at 8.5 GHz with attenuation level of -64.3 dB with -3 dB cut-off frequency at 5.6 GHz. The resonator has a smooth passband region; although it has a narrow rejection bandwidth and gradual response in the transition band.

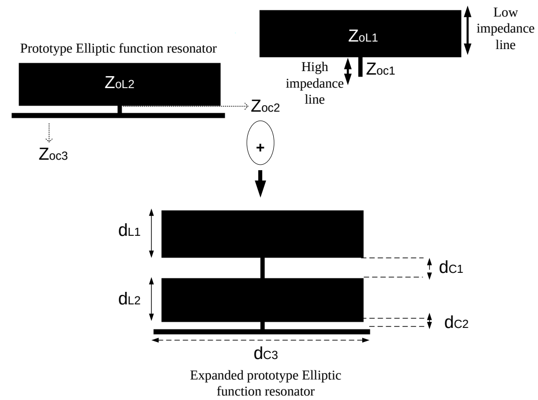

Fig. 1. The layout implementation procedure for the proposed expanded prototype Elliptic function resonator.

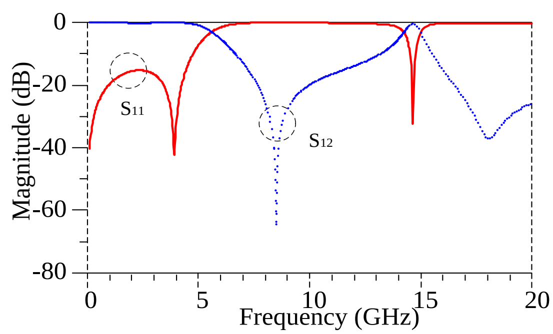

Fig. 2. Simulated S-parameters of the proposed expanded prototype Elliptic function resonator.

For this structure, the LC model for the proposed resonator is extracted as shown in Fig. 3. In this model, C represents the overall capacitance of low impedance stubs (Z_{0L1}, Z_{0L2}) respect to ground; L1 represents the overall inductance of high impedance lines (Z_{0C1}, Z_{0C2}); L represents the inductance of high impedance line of Z_{0C3}.

A comparison of the S21 parameters of this model and layout is shown in Fig. 4. The values of the lumped elements are illustrated in this figure, which are the conventional values of an Elliptic function 3 order resonator with -3 dB cut off frequency at 5.6 GHz. Transfer function for the calculation of the first transmission zero has been extracted using the proposed LC model as below:

$$T(s) = \frac{(9.793\times10^{9})S^2 + 2.789\times10^{31}}{S^3 + (3.398\times10^{10})S^2 + (1.539\times10^{21})S + 2.789\times10^{31}}. \tag{8}$$

In this equation, the coefficients of the polynomials of the numerator and denominator depends on the capacitances and inductances values of the LC model and the location of transmission zero can be adjusted by changing these values. For example, as seen in Fig. 5, by increasing the lengths of d_{L1} and d_{L2} from 1 mm to 1.5 mm, due to increment of the capacitance of C, which is the total capacitance of Z_{OL1} and Z_{OL2}, first transmission zero moves from 8.4 GHz to 7.2 GHz. Also, by decreasing the lengths of d_{L1} and d_{L2} from 1mm to 0.5 mm, due to decrement of the capacitance of C, first transmission zero moves to 11.4 GHz.

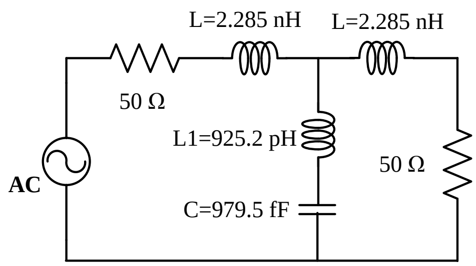

Fig. 3. The LC model for the proposed resonator.

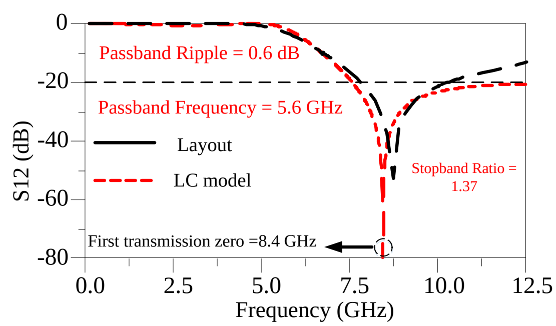

Fig. 4. A comparison of the S21 parameters of LC model and layout of the proposed resonator.

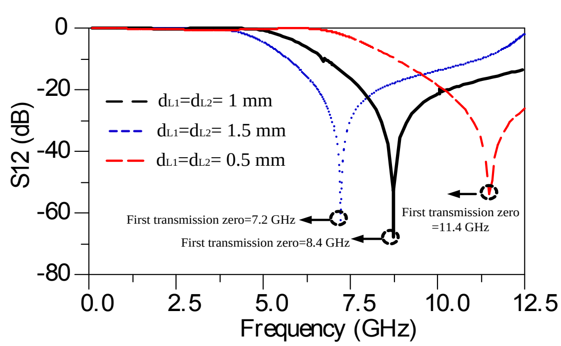

Fig. 5. Simulated S21 parameter of the proposed resonator as a function of d_{L1} and d_{L2}.

To modify the frequency response, another resonator can be cascaded to the previous one with the same dimensions as shown in Fig. 6. These dimensions are as follows: W = 1 mm, W1 = 1.1 mm, d = 4.8 mm, d2 = 0.5 mm and d3 = 11 mm. Using Equation (7), the ABCD matrix for the proposed cascaded resonator can be written as:

$$\begin{bmatrix} A & B \\ C & D \end{bmatrix} = \begin{bmatrix} 1+Z_{oc3}Y_T & Z_{oc3} \\ Y_T & 1 \end{bmatrix} \times \begin{bmatrix} 1+Z_{oc3}Y_T & Z_{oc3} \\ Y_T & 1 \end{bmatrix}. \tag{9}$$

The simulated S12-parameter of the proposed cascaded resonator is shown in Fig. 7. As seen, by moving the existence transmission zero to the lower frequency at 6.8 GHz and creating a new transmission zero at 10.7 GHz; the -3 dB cut-off frequency moves to 5 GHz with sharper transition band. Also, wider rejection band can be obtained. It has a stopband bandwidth from 5.9 GHz to 13 GHz for the attenuation level of -20 dB. But, the rejection band is so narrow yet. To extend the stopband width enough, the proposed cascaded resonator can be improved by adding another resonator, symmetrically with same dimensions as the proposed filter, as shown in Fig. 8. Thus, the stopband bandwidth has been improved up to 157% of the previous rejection band. Also, two stubs are added to the feeding lines at input and output to match the proposed filter to 50 Ω coaxial line. The ABCD matrix for the proposed cascaded symmetric resonator can be written using symmetric rules for impedances and with considering Equation 9 as:

$$\begin{bmatrix} A & B \\ C & D \end{bmatrix} = \begin{bmatrix} 1+2Z_{oc3}Y_{Ts} & 2Z_{oc3} \\ Y_{Ts} & 1 \end{bmatrix} \begin{bmatrix} 1+2Z_{oc3}Y_{Ts} & 2Z_{oc3} \\ Y_{Ts} & 1 \end{bmatrix}, \tag{10}$$

where, $Y_{Ts} = {}^{1}/_{2}\,(Y_{oc1} + Y_{oc2}) + 2(Y_{oL1} + Y_{oL2})$.

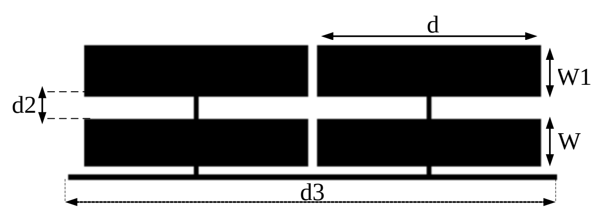

Fig. 6. The proposed cascaded resonator.

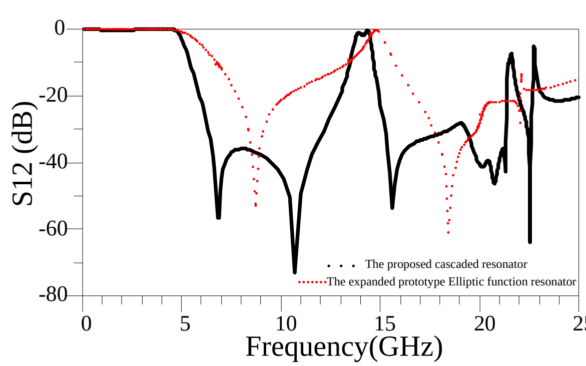

Fig. 7. The simulated S12-parameter of the proposed cascaded resonator.

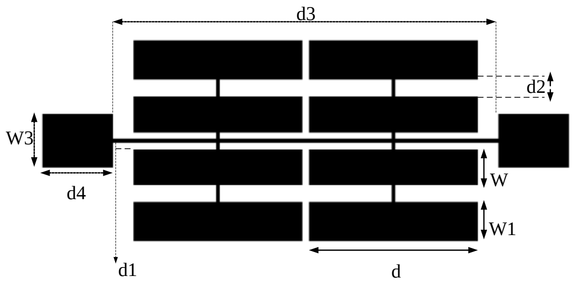

Fig. 8. The layout of the proposed LPF.

III. RESULTS

The designed LPF has been fabricated on RT/Duriod5880 substrate with dielectric constant (ε_r) of 2.22, the thickness of 0.508 mm and the loss tangent of 0.0009 and is illustrated in Fig. 9. The mentioned dimensions in the Fig. 8 are determined using equations (1-10) and tuned using ADS as a tuning tool. These dimensions are as follows: W = 1 mm, W1 = 1.1 mm, W2 = 0.1 mm, W3 = 1.5 mm, d = 4.8 mm, d1 = 0.2 mm, d2 = 0.5 mm, d3 = 11 mm and d4 = 2 mm. The measurements are done using HP8757A network analyzer. The simulated and measured S-parameters of the fabricated LPF are shown in Fig. 10. As seen, the -3 dB cut-off frequency is placed at 4 GHz. The rejection band is extended from 5 to 23.3 GHz with corresponding attenuation level of 16.6 dB. Also, the return loss is about 0 dB in the more space of the rejection band. The maximum insertion loss in the 90% of the passband region is 0.1 dB, where the maximum return loss is 15.6 dB. The physical size of the fabricated circuit, which occupies very small area, is only 11 mm × 5.5 mm = 60.5 mm^2 ($0.197\lambda_g \times 0.098\lambda_g$), where λ_g is the guided wave length at -3 dB cut-off frequency. A comparison between the characteristics of the proposed LPF and some referred works are shown in Table 1. In this table, RL (dB) and IL (dB) are the maximum return loss and insertion loss in the passband region, respectively.

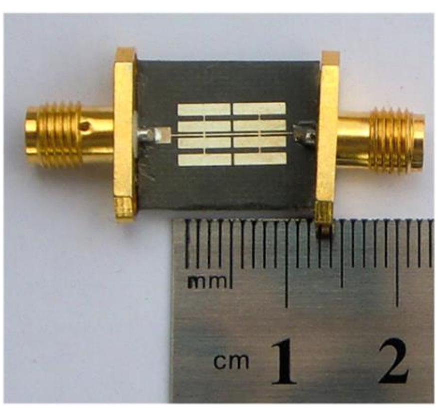

Fig. 9. Photograph of the fabricated LPF.

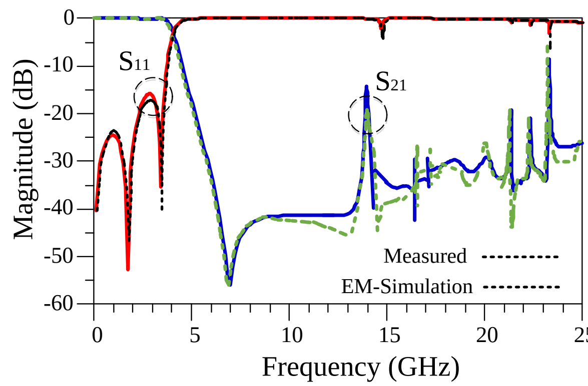

Fig. 10. The simulated and measured S-parameters of the fabricated LPF.

As can be seen in Table 1, the proposed LPF has the smallest size (60.3 mm) and the best insertion loss (0.1) among the referred filters. The good specifications of the rejection band and the small size are the important factors, which show that the proposed filter can be used in compact modern high frequency circuits as a suppressing cell in order to suppress the unwanted harmonics and interferences. The group delay of a microwave filter has a relationship to the insertion loss of a filter and design of a filter with flat group delay in the passband region is desirable [18-24]. As seen in Fig. 11, maximum variation of the measured group delay in the passband has not a significant variation and has a dispensable value and is only 0.23 ns. Table 2 shows a comparison between the maximum variation of the measured group delay in the passband for the proposed LPF and some referred works with reported group delay. As illustrated, the proposed filter has the best performance in the case of group delay.

Table 1: Performance comparisons between the proposed LPF and some referred works

Ref.	f_c (GHz)	SF	SBW/ f_c	Size (mm^2)	RL dB	IL (dB)
2	5.45	2	5.7	221	15	0.12
3	2	1	8.4	482	10	1.00
4	1.78	2	2.8	643.7	~10	0.30
5	1.67	1	5.9	100	12	0.50
6	1	2	4.1	638.4	20	0.40
12	1.18	1.5	5.9	174.2	-	-
13	1.5	2	12.1	364	20	0.13
14	3.6	2	1.9	59.8	~15	0.11
15	2.4	2	2.2	284	17	0.30
16	1.5	1.5	0.9	269	10	-
17	4.16	2	3	83.7	11	0.11
18	2.3	2	9.5	169.1	~10	1.80
This work	4	1.6	4.6	60.5	~15	0.10

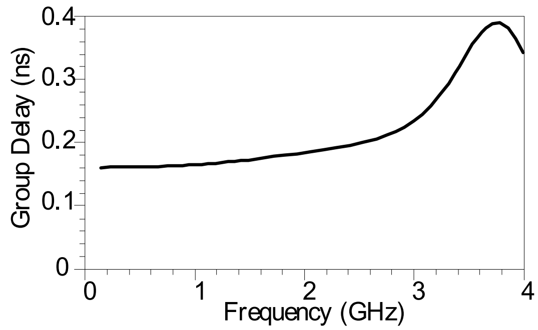

Fig. 11. The measured group delay in the passband for the proposed LPF.

Table 2: A comparison between the maximum variations of the measured group delay between some referred works with reported group delay

Ref	*f*c (GHz)	Maximum Variation of the Group Delay in the Passband (ns)	Resonator Structure
19	1.1	0.5	Tapered
20	1.74	0.5	Butterfly-shaped
21	1.55	0.5	Semi-circle stepped impedance
22	3.55	0.4	Spiral
23	2.37	0.44	Stub loaded semi-circle stepped-impedance
24	4	0.27	T-Shaped, patch and stepped impedance
This work	4	0.23	Stepped impedance

IV. CONCLUSION

A miniaturized LPF has been proposed with wide rejection band as a small size and efficient suppressing cell. The proposed LPF rejects the spurious signals from 5 GHz to 23.3 GHz with attenuation level of 16.6 dB. The maximum variation of the measured group delay in the passband region is only 0.23 ns, which is the less value in comparison with some reported works. The measurement results clear the accuracy of the simulations.

REFERENCES

[1] S. Majidifar, "High performance microstrip LPFs using dual taper loaded resonator," *Optik-International Journal for Light and Electron Optics*, vol. 127 no. 6, pp. 3484-3488, Mar. 2016.

[2] M. Hayati and F. Shama, "Compact microstrip low-pass filter with wide stopband using symmetrical U-shaped resonator," *IEICE Electronics Express*, vol. 9, no. 3, pp. 127-132, Feb. 2012.

[3] F. Wei, L. Chen, and X. Shi, "Compact lowpass filter based on coupled-line hairpin unit," *Electronics Letters*, vol. 48, no. 7, pp. 1, Mar. 2012.

[4] M. Hayati and A. Lotfi, "Elliptic-function lowpass filter with sharp cutoff frequency using slit-loaded tapered compact microstrip resonator cell," *Electronics Letters*, vol. 46, no. 2, pp. 143-144, Jan. 2010.

[5] X. B. Wei, et al., "Compact wide-stopband lowpass filter using stepped impedance hairpin resonator with radial stubs," *Electronics Letters*, vol. 47, no. 15, pp. 1, July 2011.

[6] L. Lin, Z. Li, and J. Mao, "Compact lowpass filters with sharp and expanded stopband using stepped impedance hairpin units," Microwave and *Wireless Components Letters IEEE*, vol. 206, pp. 310-312, June 2010.

[7] W. Jiacheng, "Compact quasi-elliptic .microstrip lowpass filter with wide stopband," *Electronics Letters*, vol. 46, no. 20, pp. 1384-1385, Sep. 2010.

[8] J. Wang and G. Zhang, "Design of microstrip lowpass filter with compact size and ultra-wide stopband," *Electronics Letters*, vol. 48, no. 14, pp. 856-857, July 2012.

[9] G. Lefei, J. P. Wang, and Y. Guo, "Compact microstrip lowpass filter with ultra-wide stopband," *Electronics Letters*, vol. 46, no. 10, pp. 689-691, May 2010.

[10] M. Hayati, F. Shama, and H. Abbasi. "Compact microstrip lowpass filter with wide stopband and sharp roll-off using tapered resonator," *International Journal of Electronics*, vol. 100, no. 12, pp. 1751-1759, Dec. 2013.

[11] V. Vamsi Krishna and S. Sanyal, "Sharp roll-off lowpass filter with wide stopband using stub-loaded coupled-line hairpin unit," *Microwave and Wireless Components Letters, IEEE*, vol. 21, no. 6, pp. 301-303, June 2011.

[12] M. Hayati, H. Asadbeigi, and A. Sheikhi, "Microstrip lowpass filter with high and wide rejection band," *Electronics Letters*, vol. 48, no. 19, pp. 1217-1219, Sep. 2011.

[13] M. Hayati, H. Abbasi, and F. Shama, "Microstrip lowpass filter with ultrawide stopband and sharp roll-off," *Arabian Journal for Science and Engineering*, vol. 39, no. 8, pp. 6249-53, Aug. 2014.

[14] M. Hayati, S. Roshani, S. Roshani, and F. Shama, "A novel miniaturized Wilkinson power divider with n th harmonic suppression," *Journal of Electromagnetic Waves and Applications*, vol. 27, no. 6, pp. 726-735, Apr. 2013.

[15] J. Yang and W. Wu. "Compact elliptic-function low-pass filter using defected ground structure," *Microwave and Wireless Components Letters IEEE*, vol. 18, no. 9, pp. 578-580, Sep. 2008.

[16] J. P. Wang, L. Ge, Y. X. Guo, and W. Wu, "Miniaturized microstrip lowpass filter with broad

stopband and sharp roll-off," *Electronics Letters*, vol. 46, no. 8, pp. 573-575, Apr. 2010.

[17] M. Hayati and A. Lotfi, "Compact lowpass filter with high and wide rejection in stopband using front coupled tapered CMRC," *Electronics Letters*, vol. 46, no. 12, pp. 846-848, June 2010.

[18] G. Karimi, et al., "Design of modified Z-shaped and T-shaped microstrip filter based on transfer function analysis," *Wireless Personal Communications*, vol. 82, no. 4, pp. 2005-2016, 2015.

[19] M. Hayati, F. Shama, and H. Abbasi, "Compact microstrip lowpass filter with wide stopband and sharp roll-off using tapered resonator," *International Journal of Electronics*, vol. 100, no. 12, pp. 1751-1759, Dec. 2013.

[20] M. Hayati, G. Hajian, F. Shama, and M. Shahbazitabar, "A novel microstrip lowpass filter with ultra-wide stopband using butterfly-shaped resonator," *Caspian Journal of Applied Sciences Research*, vol. 1, no. 13, Dec. 2012.

[21] M. Hayati and A. Sheikhi, "Design of wide stopband lowpass filter with sharp roll-off," *IEICE Electronics Express*, vol. 8, no. 16, pp. 1348-1353, Aug. 2011.

[22] M. Hayati and A. Sheikhi, "Compact lowpass filter with ultra-wide stopband using novel spiral compact microstrip resonant cell," *IEICE Electronics Express*, vol. 8, no. 13, pp. 1028-1033, July 2011.

[23] M. Hayati and A. Sheikhi, "Microstrip lowpass filter with very sharp transition band and wide stopband," *ETRI Journal*, vol. 33, no. 6. pp. 981-984, Dec. 2011.

[24] M. Hayati and A. Sheikhi, "Microstrip lowpass filter with very sharp transition band using T-shaped, patch and stepped impedance resonators," *ETRI Journal*, vol. 35, no. 3, pp. 538-41, June 2013.

Mohsen Hayati received the Ph.D. degrees in Electronics Engineering from Delhi University, Delhi, India, in 1992. He is currently a Professor in the Electrical Engineering Department, Razi University, Kermanshah, Iran. He has authored or co-authored over 165 papers published in international, domestic journals and conference proceedings. His current research interests include microwave and millimeter-wave devices and circuits, application of computational intelligence, artificial neural networks, fuzzy systems, neurofuzzy systems, electronic circuit synthesis, and modeling and simulations.

Farzin Shama is currently working toward the Ph.D. degree in Electrical Engineering in Razi University, Kermanshah, Iran. His research interests include the microwave engineering, and passive and active circuits design. He has been selected as top student of Iran, awarded by First Vice President of Iran in 2015.

Milad Ekhteraei is currently working toward the Ph.D. degree in Electrical Engineering in Azad University, Kermanshah, Iran. His research interests include design and analysis of the microstrip filters, and antennas.